Desalination and Water Treatment
www.deswater.com

doi: 10.5004/dwt.2023.29701

300 (2023) 12–19
July

Numerical simulation for the influence of water inlet types and inlet velocities on the hydraulic characteristics of a horizontal sedimentation tank

Ch. Yang, W. Wei*, Y. Hong, Q. Zhang, An. Ma, P. Zhang

State Key Laboratory of Eco-hydraulics in Northwest Arid Region of China, Xi'an University of Technology, Xi'an, Shaanxi 710048, China, Tel.: +86 15596886263; email: wei_wenli@126.com (W. Wei), Tel.: +86 17855598506; email: Yang_Ch2021@126.com (Ch. Yang), Tel.: +86 18149410089; email: Y_Hong2019@126.com (Y. Hong), Tel.: +86 13259176528; email: Zhang_Q2021@126.com (Q. Zhang), Tel.: +86 15690861159; email: Ma-An2021@126.com (An. Ma), Tel.: +86 13991987708; email: Peizhang@126.com (P. Zhang)

Received 17 February 2023; Accepted 17 June 2023

ABSTRACT

The effects of different water inlet types and inlet velocities on the hydraulic characteristics of a horizontal sedimentation tank was simulated by the numerical solution of gas–liquid two-phase flow model along with the realizable k–ε turbulence model. Free water surface was tracked by using the volume of fluid method, the governing equations were discretized by the finite volume method, and the coupling between velocity and pressure was solved by the Pressure implicit splitting operator algorithm. The results show that: (1) for the design of the water inlet type of a horizontal sedimentation tank, the arrangement of one inlet hole in the middle of the vertical inlet-wall can effectively reduce the size of the circulation area and improve the operation efficiency of the sedimentation tank; (2) with the total height of the inlet being fixed, reducing the height of a single inlet hole and increasing the number of inlet holes can further reduce the size of the circulation zone; in addition, the velocity fields on the cross-sections near the inlet holes become more uniform; (3) a suitable inlet velocity should be determined so as to effectively improve the hydraulic characteristics of the horizontal sedimentation tank. The research results have a certain reference value for the optimal design of similar horizontal sedimentation tanks.

Keywords: Numerical simulation; Hydraulic characteristics; Turbulence model; Volume of fluid; Horizontal sedimentation tank

1. Introduction

The horizontal and radial sedimentation tanks, as important structures in wastewater treatment, have been widely used for the removal of suspended solids and the sludge sedimentation after biochemical treatment. The research on the sedimentation tanks mainly focuses on the influence of suspended solids in wastewater on the removal efficiency and focuses on the method to effectively improve the sedimentation performance [1,2]. But the design and operation of sedimentation tanks are the two main factors affecting their sedimentation efficiency [3], therefore, many scholars have studied something about them.

The hydraulic characteristics and solid settlement characteristics in sedimentation tanks have been studied by using mathematical models. The Lagrangian method (discrete phase model) was used to simulate the three-dimensional (3D) fluid dynamics and flow characteristics in a sedimentation tank by considering the momentum exchange between solid–liquid two phases [4]. In order to analyze the sediment concentration distribution more accurately, Zhang et al. [5] established the suspended sediment transport model, and used it to simulate the concentration distribution in a sedimentation tank, which shows that the simulated concentration distribution of each monitoring section is basically consistent with the experimental

* Corresponding author.

values. Tarpagkou and Pantokratoras [6], the dynamics and the structure of flow in a rectangular sedimentation tank were numerically simulated, by which the effect of the plate settler on the process efficiency was evaluated; and a conclusion was made that, compared with the previous design, the plate settler can improve the internal flow fields of the sedimentation tank and increase its sedimentation efficiency by 20%. Gao and Stenstrom [7], the performance of three turbulence models of the standard *k*–ε model, the renormalized group (RNG) *k*–ε model and the realizable *k*–ε model, was evaluated by studying the hydrodynamics and solid distribution near the bottom of a sedimentation tank, and the results show that three turbulence models have nearly the same prediction of suspended solids concentration near the outlet, but have a significantly different prediction near the inlet and in the sludge hopper.

The baffle of sedimentation tank has a great influence on the hydraulic characteristics and sedimentation efficiency. Shahrokhi et al. [8,9], the flow velocities were measured and simulated in a rectangular primary sedimentation tank with arranging different numbers of fixed-length baffles, and the results show that the reasonable number of the baffles in appropriate positions can effectively reduce the volume size of the recirculation zone, and reduce the turbulent kinetic energy so as to improve the operation efficiency of the sedimentation tank. Wei et al. [10], the effects of two vertical baffles with different lengths near the inlet on the liquid–solid two-phase flow characteristics in a radial flow secondary sedimentation tank were simulated, which shows that the used long baffles can make the flow field be more conducive to rapid sedimentation of sludge. Rostami et al. [11], a two-dimensional (2D) single-phase flow model was used to simulate the streamlines, size of recirculation zone, and the turbulent kinetic energy in a primary sedimentation tank, and the results show that different inlet positions have a great influence on the flow patterns of the sedimentation tank, and that increasing the number of inlets can effectively reduce the turbulent kinetic energy near the inlet zone and produce uniform flow. Asgharzadeh et al. [12], the influence of baffle configuration on the velocity and concentration distribution of a rectangular sedimentation tank was studied by an experiment method. It concludes that the operation efficiency of the sedimentation tank can be effectively improved by placing an appropriate height of baffle in the middle of the recirculation area.

The design parameters and inlet velocity have a great influence on the hydraulic characteristics and sedimentation efficiency of a horizontal flow sedimentation tank. Therefore, the flow fields of an advection sedimentation tank with different inlet flow velocities were simulated by the study of Liu [13], and then the velocity distributions on the characteristic sections were analyzed, which shows that greater inlet flow velocity is not conducive to producing uniform flows, while the installed diversion baffles in transition zone can improve the uniformity of flows in a sedimentation tank. Patziger et al. [14], the effect of water inlet geometry on a sedimentation tank was studied, the results show that a reasonable inlet form can significantly improve the efficiency of sewage sludge treatment. In order to treat a larger wastewater volume, Rodríguez López et al. [15] studied the relationship between the hydrodynamic characteristics and the inlet flow rate of a pilot scale sedimentation tank, and found that the flow conditions of sedimentation can be improved by changing the water inlet layout.

In practice, the wastewater treatment efficiency of a sedimentation tank is affected by its internal hydraulic characteristics, and the hydraulic characteristics are mainly affected by the design parameters, sewage inlet form, inflow velocity, and the number, size and position of baffles [1–15]. The above literatures have studied these problems, but lack the research on the water inlet form of a sedimentation tank. Therefore, by using a numerical simulation method with volume of fluid (VOF) and realizable *k*–ε model, the influence of different water inlet forms and inlet velocities was studied on the hydraulic characteristics of a horizontal sedimentation tank.

2. Mathematical model

2.1. Governing equations

The Reynolds averaged Navier–Stokes (N-S) equations are always closed by the turbulence models, such as the standard *k*–ε model, and the relatively improved models named by the RNG *k*–ε and realizable *k*–ε models in computational fluid dynamics (CFD) [16–18]. The realizable *k*–ε model can well simulate the flow fields with bend streamlines [19]. Therefore, the realizable *k*–ε model was used to close the Reynolds-averaged N-S equations describing the flows in horizontal sedimentation tanks. The governing equations [20,21] are written as follows:

$$\frac{\partial \rho}{\partial t}+\frac{\partial\left(\rho u_i\right)}{\partial x_i}=0 \tag{1}$$

and

$$\frac{\partial\left(\rho u_i\right)}{\partial t}+\frac{\partial\left(\rho u_i u_j\right)}{\partial x_j}=-\frac{\partial p}{\partial x_i}+\frac{\partial}{\partial x_j}\left[\mu\left(\frac{\partial u_i}{\partial x_j}+\frac{\partial u_j}{\partial x_i}\right)\right]-\frac{\partial}{\partial x_j}\left(\rho\overline{u_i' u_j'}\right)+\rho g_i \tag{2}$$

where ρ is density; t is time; x_i is the space coordinate in i direction; p is pressure; μ is molecular kinematic viscosity; g_i is the gravitational acceleration in i direction; u_i and u'_i are the time-averaged and fluctuating velocity components in i direction, respectively; and the subscripts i, j = 1, 2, 3.

The Reynolds stress term, $-\rho\overline{u_i' u_j'}$, in Eq.(2), is often modeled by the Boussinesq hypothesis relating these stresses to the mean deformation rates and mean velocity gradients [20], and can be written as:

$$-\rho\overline{u_i' u_j'}=\mu_t\left(\frac{\partial u_i}{\partial x_j}+\frac{\partial u_j}{\partial x_i}\right)-\frac{2}{3}\left(\rho k+\mu_t\frac{\partial u_i}{\partial x_i}\right)\delta_{ij} \tag{3}$$

where μ_t is the turbulent viscosity; k is the turbulent kinetic energy of fluid per unit mass; δ_{ij} is the Kronecker function, with $\delta_{ij}=1(i=j)$ and $\delta_{ij}=0(i\neq j)$.

In the realizable k–ε turbulence model, the transport equations for k and ε are given by the study of Wei et al. [20,21]:

$$\frac{\partial(\rho k)}{\partial t}+\frac{\partial(\rho k u_i)}{\partial x_i}=\frac{\partial}{\partial x_j}\left[\left(\mu+\frac{\mu_t}{\sigma_k}\right)\frac{\partial k}{\partial x_j}\right]+G_k-\rho\varepsilon \tag{4}$$

and

$$\frac{\partial(\rho\varepsilon)}{\partial t}+\frac{\partial(\rho\varepsilon u_i)}{\partial x_i}=\frac{\partial}{\partial x_j}\left[\left(\mu+\frac{\mu_t}{\sigma_\varepsilon}\right)\frac{\partial\varepsilon}{\partial x_j}\right]+\rho C_1 E\varepsilon-\rho C_2\frac{\varepsilon^2}{k+\sqrt{v\varepsilon}} \tag{5}$$

where ε is the turbulent energy dissipation rate; σ_k, σε and C_2 are the empirical constants with a value of 1.0, 1.2, and 1.9, respectively; G_k is the production term of turbulent kinetic energy k; and the other parameters are:

$$C_1=\max\left(0.43,\frac{\eta}{\eta+5}\right),\eta=\left(2E_{ij}\cdot E_{ij}\right)^{1/2}\frac{k}{\varepsilon},E_{ij}=\frac{1}{2}\left(\frac{\partial u_i}{\partial x_j}+\frac{\partial u_j}{\partial x_i}\right),$$

$$\mu_t=\rho C_\mu\frac{k^2}{\varepsilon},C_\mu=\frac{1}{A_0+A_s U^* k/\varepsilon},A_0=4.0,A_s=\sqrt{6}\cos\varphi,$$

$$\varphi=\frac{1}{3}\cos^{-1}\left(\sqrt{6}W\right),W=\frac{E_{ij}E_{jk}E_{ki}}{\left(E_{ij}E_{ij}\right)^{1/2}},U^*=\sqrt{E_{ij}E_{ij}+\Omega'_{ij}\Omega'_{ij}},$$

$$\Omega'_{ij}=\Omega_{ij}-2\varepsilon_{ijk}\omega_k,\Omega_{ij}=\overline{\Omega}_{ij}-\varepsilon_{ijk}\omega_k,$$

in which E_{ij} is the time average strain rate; ω_k is the rotational rate; $\overline{\Omega}_{ij}$ is the time average rotation rate tensor; v is the average velocity.

2.2. VOF method

The VOF method [20–22] is used to track the liquid / gas interface. The volume fraction of liquid, F, is defined as the ratio of the volume occupied by liquid in a control cell to the total volume of the control cell. The value of F ranges between 0 and 1. F = 1 and F = 0 represent a control cell completely filled with liquid and gas, respectively; and 0 < F < 1 represents a control cell partly filled with liquid, which shows the interface between liquid and gas. The value of F can be obtained by solving a separate passive transport equation, which is given by Hirt and Nicholas [22]:

$$\frac{\partial F}{\partial t}+\frac{\partial(Fu_i)}{\partial x_i}=0 \tag{6}$$

The physical properties, ρ and μ, of the mixture of gas and water appearing in the transport Eqs. (1)–(5), are determined by the presence of water and air in each control volume, and can be computed by the following equations:

$$\rho=F_w\rho_w+\left(1-F_w\right)\rho_a \tag{7}$$

$$\mu=F_w\mu_w+\left(1-F_w\right)\mu_a \tag{8}$$

where ρ_a and μ_a are the density and viscosity of air, respectively; ρ_w and μ_w are the density and viscosity of water, respectively.

3. Physical model and boundary conditions

3.1. Layout of inlet positions

The physical model is a 2.5-m long, 0.5-m wide, and 0.5-m high rectangular sedimentation tank with a water depth of 0.34 m. In order to study the influence of wastewater inlet type on the hydraulic characteristics of the horizontal sedimentation tank, 5 different water inlet types, cases (a)–(e) in Fig. 1, are considered. Cases (a)–(c) have only one inlet hole with a height of 0.1 m, and the inlet hole is respectively arranged at different water depth in the vertical solid wall: case (a) near the water surface, case (b) at half of the water depth, and case (c) near the bottom of the sedimentation tank; case (d) has two inlet holes with a height of 0.05 m, and the two inlet holes are evenly arranged at 1/3 and 2/3 of the water depth; and case (e) has three inlet holes, respectively with a height of 0.04, 0.02, and 0.04 m, and are equally spaced in the vertical solid wall.

3.2. Calculation region and grid generation

The 2D numerical simulation was used for the study of the horizontal flow sedimentation tank. The calculation region with a water depth of 0.34 m is 2.5 m long and 0.5 m high. By taking case (a) as an example, as shown in Fig. 2a, Gambit software was used for its grid generation and the whole region was divided into rectangular meshes. The 5 types of rectangular grids with a size of 4, 6, 8, 10, and 12 mm, were respectively used for the simulation to analyze the effect of different mesh densities on grid independence, which shows that the rectangular grid with a length of 8 mm, as shown in Fig. 2b, meets the requirement of grid independence. The 5 cases (a)–(e) use the same grid in Fig. 2b for the simulations.

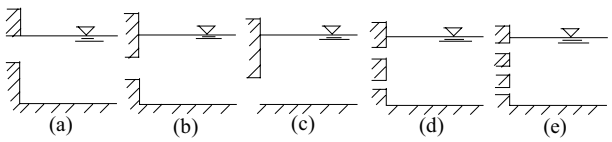

Fig. 1. Arrangement of water inlet types.

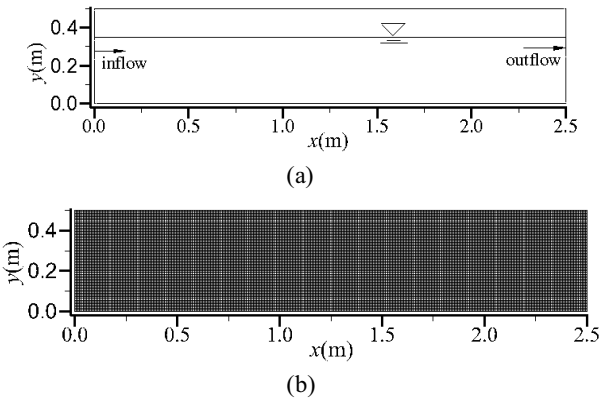

Fig. 2. Computational region and grid: (a) 2D region and (b) 2D grid.

3.3. Boundary conditions

At the inlet boundary, the water inlet velocity value was given, and at the outlet boundary the pressure outlet condition was given; and the top boundary is connected with the atmosphere, at which the relative pressure was given as 0. The turbulence intensity at the inlet and outlet were set. The bottom and side walls (including baffles) are taken as solid walls, and their boundary condition was determined by the standard wall-function method.

4. Results and analysis

4.1. Effects of different inlet types on the hydraulic characteristics

4.1.1. Analysis of streamline distributions under the 5 cases

For the 5 cases (a)–(e) in Fig. 3 with a water inlet velocity value of 0.035 m/s, the streamline distributions show that there are quite different sizes and shapes of recirculation zones near the water inlets. The recirculation zones are the 'dead water zone'; therefore, it affects the effective capacity of the sedimentation tank, and then decreases its treatment efficiency.

It can be seen from Fig. 3 that, there is a large recirculation zone with a length close to 0.8 m for case (a); and a recirculation zone, respectively above and below the water inlet for case (b), and the length close to 0.6 m of the below is larger than the above; and a larger recirculation zone appears above the water inlet for case (c), and the streamlines at the right-hand side of the recirculation zone go up, and then a new recirculation zone is generated under the main flow; the total length of the two recirculation zones is close to 1.0 m. Comparing the streamlines of cases (a)–(c), it can be seen that when only one inlet hole is arranged for the horizontal sedimentation tank, its position set in the middle, as shown in case (b), can effectively reduce the size of the recirculation area, and the length of the recirculation area is reduced to 60% of the maximum value of case (c), which can improve the operation efficiency of the horizontal sedimentation tank.

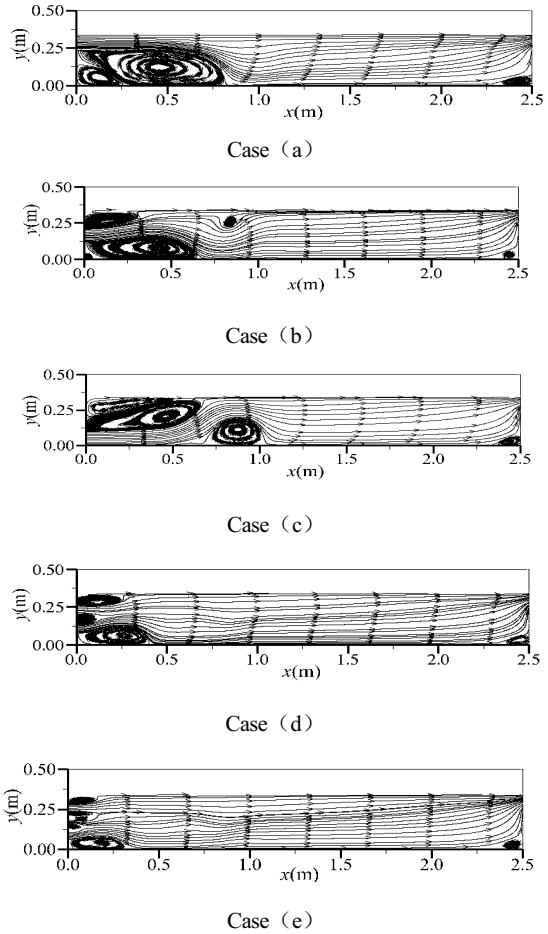

Fig. 3. Streamline distributions under 5 cases (a)–(e).

For case (d) in Fig. 3, three small recirculation zones appear near the inlet holes, and the biggest length of recirculation zone is close to 0.4 m. The size of recirculation zone is significantly reduced compared with the three cases (a)–(c), and the length of recirculation zone is reduced to 40% of the maximum value of case (c). However, the size of recirculation zone for case (e) is further reduced, and its length is reduced to 30% of the maximum value of case (c), and is significantly smaller than that of case (d). Compared with cases (b), (d), and (e), when the total height of the water inlet holes is the same, the more the number of water inlet holes is, the smaller is the size of the recirculation zone in the sedimentation tank, and thus the more uniform is the streamline distribution near the water inlet holes. Therefore, with the same total height of the water inlet holes, the recirculation area in the sedimentation tank can be effectively reduced by reducing the height of a single water inlet hole and increasing the number of water inlet holes.

4.1.2. Analysis of the velocity vector distributions under the 5 cases

In addition, by comparing the velocity vector distributions of the 5 cases (a)–(e) in Fig. 4, it can be seen that the high-speed flow near the water inlet is in the surface layer under case (a), in the middle layer under case (b), and in the bottom layer under case (c). The flow field distributions in the region near the inlet holes of the sedimentation tank under the 3 cases (a)–(c) are much uneven, thus, the velocity gradient along the cross-sections changes greatly, which is not conducive to sedimentation of solid particles. It can be seen from the velocity vector distributions of cases (d) and (e) that, with an increase in the number of inlet holes, the velocity distributions on the cross-sections become more uniform. Such velocity field is conducive to sedimentation of solid particles, and improve the operation efficiency of the horizontal sedimentation tank.

4.2. Effects of different inlet velocities on the hydraulic characteristics

The inlet velocity of primary sedimentation tank is an important factor affecting the operation efficiency of sedimentation; therefore, a reasonable inlet velocity should be determined. We take case (a) (in Section 4.1 – Analysis of the velocity vector distributions under the 5 cases) as an example to study the effects of different inlet velocities on

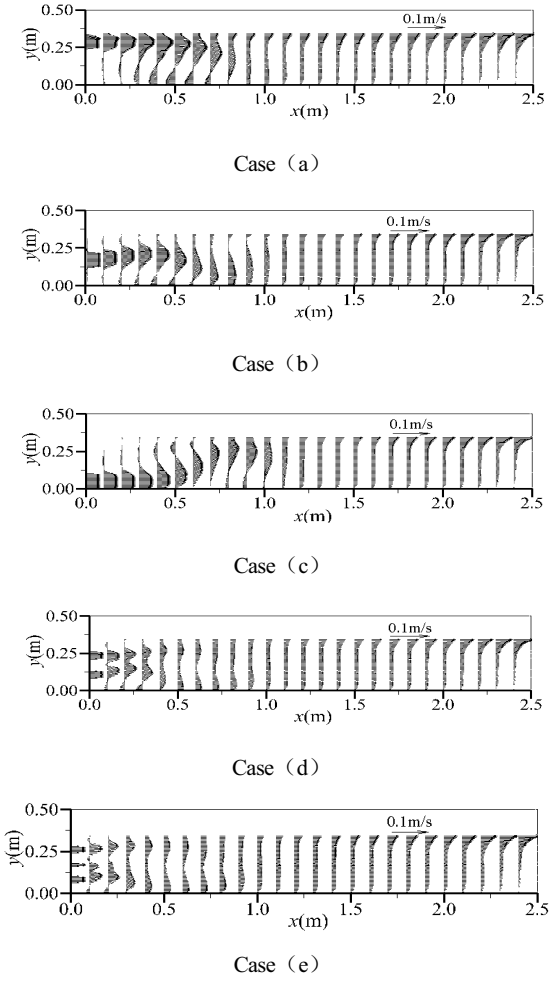

Fig. 4. Vector distributions under 5 cases (a)–(e).

the hydraulic characteristics. The 5 different inlet velocity values of 0.015, 0.025, 0.035, 0.045, and 0.055 m/s are given for the simulations, and the calculation region, grid division, the other boundary conditions, and solution method are the same as that in Section 4.1 – Analysis of the velocity vector distributions under the 5 cases.

4.2.1. Analysis of the streamline distributions under 5 different values of inlet velocity

The simulated streamline distributions under the 5 different values of inlet velocity are shown in Fig. 5. It can be seen from Fig. 5a that, with an inlet velocity given as 0.015 m/s, at the left-hand side of the tank there is a recirculation area with a length of about 0.56 m below the inlet streamlines; and at the right-hand side a larger recirculation area with a length of about 0.9 m appears below the outlet. The reason is that, too small inlet velocity results in a very small flow velocity field in the whole flow region, and the small flow velocity field along with the fluid viscosity easily produces recirculation zone forming a "dead water zone"; therefore, the effective volume of the sedimentation tank is reduced, and the treatment efficiency of the tank is decreased.

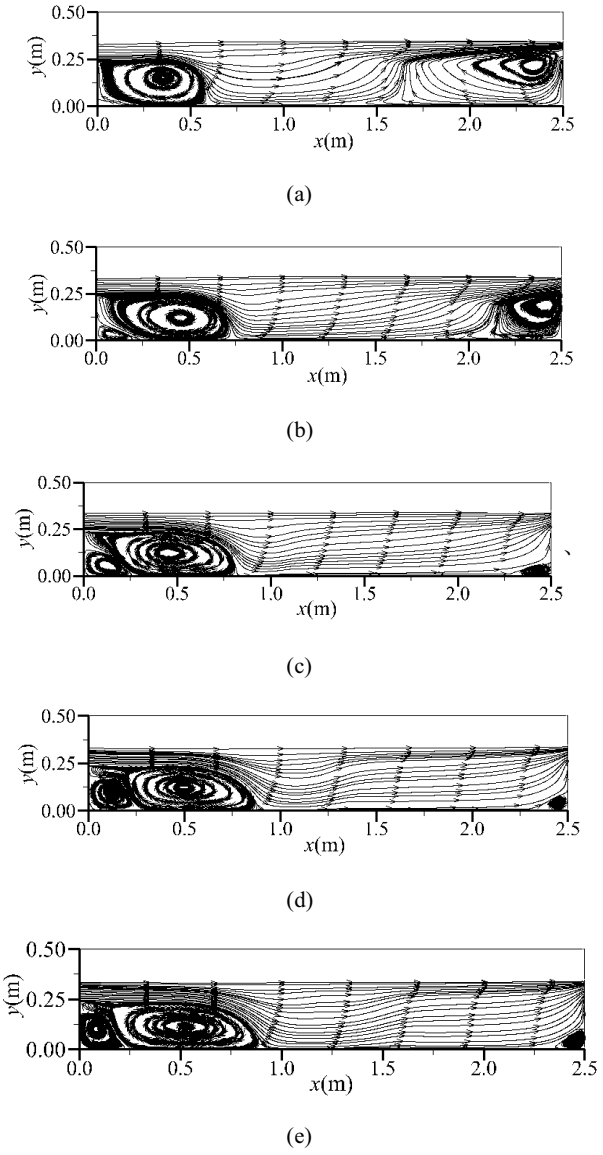

Fig. 5. Streamline distributions under different inlet velocities of (a) 0.015 m/s, (b) 0.025 m/s, (c) 0.035 m/s, (d) 0.045 m/s, and (e) 0.055 m/s.

In Fig. 5b, with the inlet velocity given as 0.025 m/s, the length of the recirculation zone below the inlet is about 0.7 m, while below the outlet is only about 0.35 m. In Fig. 5c, when the inlet velocity is increased as 0.035 m/s, the recirculation zone below the inlet increases to 0.8 m, while below the outlet and in the lower right corner of the sedimentation tank a very small one appears and can be ignored. It can also be seen from Fig. 5d and e that, when the inlet velocity increase to 0.045 and 0.055 m/s, the recirculation areas with a length of about 0.9 m is basically similar to that of the inlet velocity 0.035 m/s, that is, length of the recirculation area does increase with the inlet velocity of 0.045 and 0.055 m/s, compared to that of 0.035 m/s.

Fig. 5a–e show that a small inlet velocity of the sedimentation tank produces a larger recirculation area below the water outlet at the right-hand side; with a gradual

increase in the inlet velocity, the recirculation area gradually decreases. Therefore, the water inlet velocity of sedimentation tank should not be too small. With the inlet velocity greater than 0.035 m/s, the size of the recirculation zone at the right-hand side of the sedimentation tank becomes similar; therefore, the inlet velocity of 0.035 m/s is the reasonable one.

4.2.2. Analysis of the influence of inlet velocity on the sedimentation tank

The five lines 1–5 representing different cross-sections at a location of x = 0.1, 0.5, 0.9, 1.3, and 1.7 m are shown in Fig. 6; and the velocity distributions along the five lines under the different inlet velocities of 0.035, 0.045, and 0.055 m/s, are shown in Fig. 7.

It can be seen from Fig. 7a and b that, on lines 1 and 2, the higher the inlet flow rate is, the higher becomes the surface velocity of the sedimentation tank; but the velocity distribution near the bottom is similar. The higher surface velocity near the inlet will transport solid particles in sewage to the outlet of the sedimentation tank, and take the particles out from the sedimentation tank, which is not conducive to the sedimentation of suspended solid particles.

From Fig. 7c, on line 3, the velocity distributions near water surface and the bottom under different inlet velocities are similar, but at its middle region are different; the larger the inlet velocity is, the greater becomes the middle region velocity.

From Fig. 7d and e, with the different inlet velocities, the velocity distributions on lines 4 and 5 are similar in the upper fluid layer; but the higher the inlet velocity is, the higher becomes the velocity in the lower fluid layer. If the velocity at the bottom is too high, fine solid particles will be lifted up, which is not conducive to sedimentation, and reduce the treatment efficiency of the sedimentation tank. Therefore, the inlet velocity of the primary sedimentation tank should not be too large.

As stated above, Fig. 7a–e show that the inlet velocity of the sedimentation tank cannot be too small or too large. Determining a suitable inlet velocity can effectively improve the treatment efficiency. For the rectangular sedimentation tank in case (a), the suitable inlet velocity is determined to be 0.035 m/s.

5. Further study plan

Numerical simulation and experimental methods depend upon each other. Experiment is the main way to investigate a new basic phenomenon, taking a large amount of observation data as the foundation, still, the validation for a numerical simulation result must use the measured (in prototype or model) data. Doing numerical simulation in advance can obtain the preliminary results, which can make the corresponding experiment plan be more purposeful, and often reduce the number of tests needed by systematically doing experiments, and are much useful for the design of experimental device [19,20].

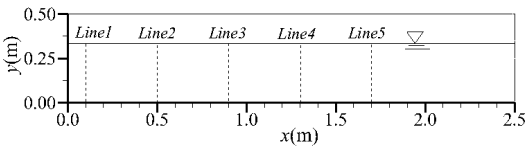

Fig. 6. Positions of the 5 lines.

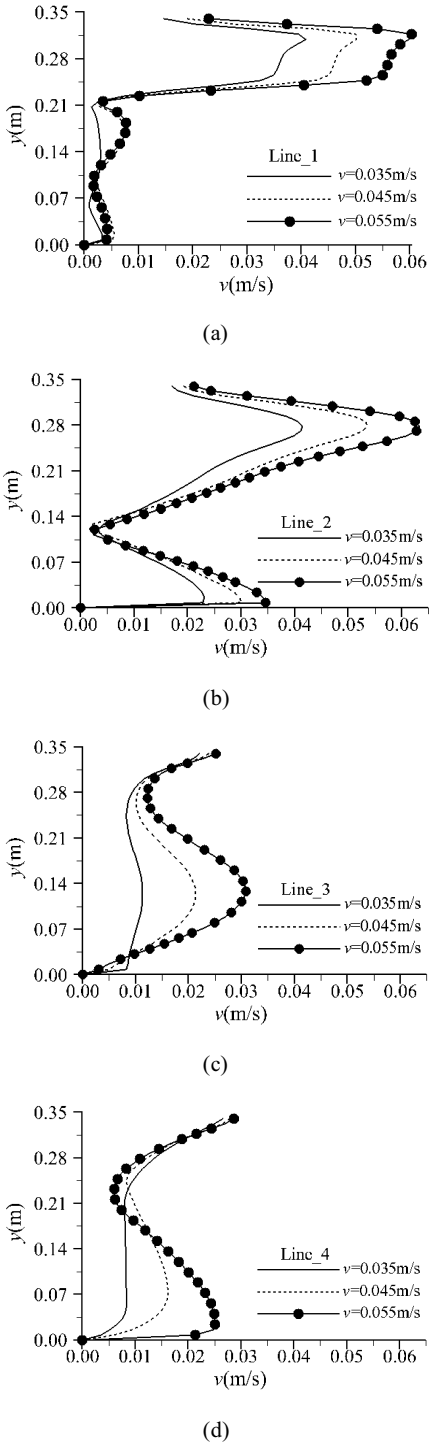

Fig. 7. Comparisons of horizontal velocity distributions along lines 1–5 under different inlet velocities: (a) line 1, (b) line 2, (c) line 3, (d) line 4, and (e) line 5.

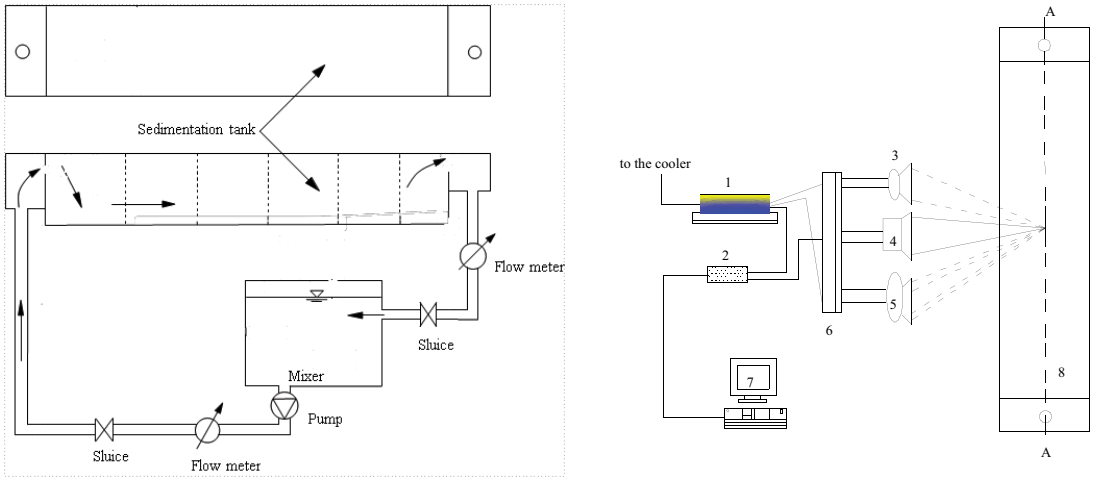

Fig. 8. Sketch of (a) experimental system and (b) measurement of particle dynamic analyzer. (1) Laser; (2) signal processor; (3) 1D fiber-optic probe; (4) receiver; (5) 2D fiber-optic probe; (6) self-motion shelf; (7) computer; (8) sedimentation tank.

Here a numerical method has been used to study the influence of water inlet types and inlet velocities on the hydraulic characteristics of a horizontal sedimentation tank. Next, further study will be done to validate the simulation model by an experimental method. Particle dynamic analyzer (PDA) will be used to the test model for the sedimentation tank. Fig. 8a shows the experimental system of the sedimentation tank. Fig. 8b shows the sketch of the principle of PDA. PDA (type 58N50) is employed to measure the flow field in the sedimentation tank. It was developed on the basis of traditional laser Doppler anemometry, composing of laser, transmitting system, receiver, signal processor, computer, as well as a 3D self-motion shelf. The different measurement sections along x-coordinate axis in the sedimentation tank are illustrated with the dashed lines in Fig. 6.

After doing experiments on the sedimentation tank, the measured velocity values will be compared with the simulated one, by which the reliability of the simulation results will be further verified. After validating the mathematical model, it will be used to predict flow fields in a similar sedimentation tank with different inlet types and inlet velocities, by which a better inlet type and inlet velocity can be obtained.

6. Conclusions

By using the CFD method to study the effects of different water inlet types and inlet velocities on the hydraulic characteristics of the horizontal sedimentation tank, the following conclusions have been made:

- When only one water inlet was arranged, its position at the middle of the vertical wall can make the length of the recirculation zone be small, and can effectively improve the operation efficiency of sedimentation.
- When the total height of the water inlet is fixed, reducing the height of a single water inlet hole and increasing the number of water inlet holes can make the size of the recirculation zone become small, and make the distributions of flow velocity fields on cross-sections become more uniform, which is conducive to the sedimentation of suspended solid particles so as to improve the operation efficiency of the sedimentation tank.
- The water inlet velocity of the sedimentation tank cannot be too small or too large; that is, a suitable inlet velocity should be determined so as to effectively improve its treatment efficiency.

Acknowledgments

Financial support of this study was from the National Natural Science Foundation of China (Grant No.51578452 and No.51178391) and the scientific research projects of Shaanxi Province (2020SF-354, 2016GY-180).

Symbols

A_0	—	Parameter with a value of 4.0 for the computation of C_μ
A_s	—	Parameter for the computation of C_μ
C	—	Parameter
C_μ	—	Parameter in Eq. (5)
C_1	—	Model parameter in Eq. (5) with a value of 1.9
C_2	—	Model parameter in Eq. (5) with a value of 1.9
E_{ij}	—	Time average strain rate for computation of C_1
F	—	Volume fraction of liquid
g_i	—	Gravitational acceleration in i-direction, i = 1, 2, and 3 m/s^2
G_k	—	Production term in Eq.(4)
k	—	Turbulent kinetic energy, m^2/s^2
p	—	Pressure, kg/m·s^2
t	—	Time, s
u_i	—	Velocity component in i-direction, i = 1, 2, and 3 m/s
u'_i	—	Fluctuating velocity component in i-direction, i = 1, 2, and 3 m/s

U^* — Parameter for computation of C_μ
v — Average velocity, m/s
W — Parameter for computation of C_μ
x_i — Space coordinate in i-direction, i = 1, 2, and 3 m

Greek

δ_{ij} — Kronecker function in Eq. (3), δ_{ij} = 1 with $i = j$, and δ_{ij} = 0 with $i \neq j$
ε — Kinetic energy dissipation rate, m^2/s^3
ε_{ijk} — Parameter for the computation of C_μ
η — Parameter for computing C_1
μ — Molecular kinematic viscosity, kg/m·s
μ_t — Turbulent kinematic viscosity, kg/m·s
ρ — Density, kg/m^3
σ_k — Parameter in Eq. (4) with a value of 1.0
σ_ε — Parameter in Eq. (5) with a value of 1.2
φ — Parameter for computation of C_μ
Ω_{ij} — Parameter for computation of C_μ
$\overline{\Omega}_{ij}$ — Time average rotation rate tensor for the computation of C_μ
ω_k — Rotational rate for the computation of C_μ

Subscripts

a — Air
i, j — Direction, i = 1, 2, and 3; j = 1, 2, and 3
t — Turbulence
w — Water

A list of abbreviations

1D — One-dimensional
2D — Two-dimensional
3D — Three-dimensional
CFD — Computational fluid dynamics
N-S — Navier–Stokes
PISO — Pressure implicit splitting operator algorithm
PDA — Particle dynamic analyzer
RNG — Renormalized group
VOF — Volume of fluid

References

[1] X. Wang, X. Sun, H. Jiang, H. Zhao, Sh. Li, Problems existing in the operation of horizontal flow sedimentation tank and their improving measures, China Water Wastewater, 22 (2006) 27–30 (in Chinese).
[2] Ch. Yan, D. Zhang, P. Lu, Zh. Li, The study and prospect of the secondary clarifier models in wastewater treatment, J. Chongqing Univ., 27 (2004) 130–133 (in Chinese).
[3] S. Arendze, M.S. Sibiya, Comparing the flow dynamics and particle settling in full scale sedimentation tanks of different lengths, Water Sci. Technol. Water Supply, 17 (2016) 998–1006.
[4] R. Tarpagkou, A. Pantokratoras, CFD methodology for sedimentation tanks: the effect of secondary phase on fluid phase using DPM coupled calculations, Appl. Math. Modell., 37 (2013) 3478–3494.
[5] W. Zhang, Z. Zou, J. Sui, Numerical simulation of a horizontal sedimentation tank considering sludge recirculation, J. Environ. Sci., 22 (2010) 1534–1538.
[6] R. Tarpagkou, A. Pantokratoras, The influence of lamellar settler in sedimentation tanks for potable water treatment—a computational fluid dynamic study, Powder Technol., 268 (2014) 139–149.
[7] H. Gao, M.K. Stenstrom, Evaluation of three turbulence models in predicting the steady state hydrodynamics of a secondary sedimentation tank, Water Res., 143 (2018) 445–456.
[8] M. Shahrokhi, F. Rostami, M.A. Md Said, S.R. Sabbagh Yazdi, Syafalni, The effect of number of baffles on the improvement efficiency of primary sedimentation tanks, Appl. Math. Modell., 36 (2012) 3725–3735.
[9] M. Shahrokhi, F. Rostami, M.A. Md Said, Syafalni, Numerical modeling of baffle location effects on the flow pattern of primary sedimentation tanks, Appl. Math. Modell., 37 (2013) 4486–4496.
[10] W. Wei, Z. Zhang, Ch. Bai, Y. Liu, Numerical simulation of a feed flow baffle on the flow of a radial sedimentation tank by using a liquid-solid two-phase model, Chin. J. Appl. Mech., 33 (2016) 93–98+183 (in Chinese).
[11] F. Rostami, M. Shahrokhi, M.A. Md Said, R. Abdullah, Syafalni, Numerical modeling on inlet aperture effects on flow pattern in primary settling tanks, Appl. Math. Modell., 35 (2011) 3012–3020.
[12] H. Asgharzadeh, B. Firoozabadi, H. Afshin, Experimental investigation of effects of baffle configurations on the performance of a secondary sedimentation tank, Sci. Iran., 18 (2011) 938–949.
[13] J. Liu, Effect of inlet-velocity on water flow distribution in horizontal flow settling tank, Eng. Constr., 49 (2017) 60–62+66 (in Chinese).
[14] M. Patziger, H. Kainz, M. Hunze, J. Józsa, Influence of secondary settling tank performance on suspended solids mass balance in activated sludge systems, Water Res., 46 (2012) 2415–2424.
[15] P. Rodríguez López, A.G. Lavín, M.M. Mahamud López, J.L. Bueno de las Heras, Flow models for rectangular sedimentation tanks, Chem. Eng. Process. Process Intensif., 47 (2008) 1705–1716.
[16] S.A. Orszag, I. Staroselsky, W.S. Flannery, Y. Zhang, Chapter 4 – Simulation and Modeling of Turbulent Flows, Introduction to Renormalization Group Modeling of Turbulence, Oxford Univ. Press Inc., New York, NY, USA, 1996.
[17] T.-H. Shih, W.W. Liou, A. Shabbir, Z. Yang, J. Zhu, A new k–ε eddy viscosity model for high Reynolds number turbulent flows, Comput. Fluids, 24 (1995) 227–238.
[18] B.E. Launder, D.B. Spalding, The numerical computation of turbulent flows, Comput. Methods Appl. Mech. Eng., 3 (1974) 269–289.
[19] W. Wei, C. Lou, Y. He, J. Wei, Y. Cai, Y. Chang, Computational fluid dynamics for the influence of a semi-circular guiding wall on the hydraulic characteristics in an oxidation ditch, Desal. Water Treat., 196 (2020) 93–101.
[20] W. Wei, Y. Liu, B. Lv, Numerical simulation of optimal submergence depth of impellers in an oxidation ditch, Desal. Water Treat., 57 (2015) 8228–8235.
[21] W.L. Wei, H.C. Dai, Turbulence Model Theory and Engineering Applications, 1st ed., Shanxi Sci. Tech. Press, Xi'an City, 2006 (in Chinese).
[22] C. Hirt, B. Nicholas, Volume of fluid (VOF) method for the dynamics of free boundaries, J. Comput. Phys., 39 (1981) 201–225.